Effect of the L-DOPA hydroxyl groups in the formation of supramolecular hydrogels

Effect of the L-DOPA hydroxyl groups in the formation of supramolecular hydrogels

Nicola Zanna,*[a] Debora Iaculli,[a] and Claudia Tomasini*[a]

[a]Dipartimento di Chimica "G. Ciamician" - Alma Mater Studiorum Università di Bologna - Via Selmi 2, 40126 Bologna (Italy)

Abstract

Fmoc-L-DOPA-D-Oxd-OH was prepared starting from commercially available L-DOPA. Its gelation ability was tested as a comparison with Fmoc-L-Tyr-D-Oxd-OH and Fmoc-L-Phe-D-Oxd-OH using ten different triggers. Among them, only GdL, $CaCl_2$ and $ZnCl_2$ form strong hydrogels with the three gelators. The analysis of the aerogels obtained by hydrogels freeze drying show that the three gelators induce always the formation of dense networks, that strongly depend on the gelator nature. The rheological analysis of these samples demonstrate that the stronger gels are obtained with the L-Tyr containing gelator, while the L-DOPA containing hydrogels are characterized by a storage modulus approximately an order of magnitude lower. Finally, the L-Phe containing gelator show a different trend respect to the other ones depending on the trigger. All the hydrogels show a thixotropic behaviour at the molecular level. These results indicate that the hydrogel formation is sensitive both to the number of the hydroxyl moieties on the aromatic rings and on the trigger nature.

Introduction

In order to understand aggregation phenomena, oligopeptides may be designed and prepared either to mimicking[1–10] or to interfere with[11–13] these processes. The non-proteinogenic amino acid 3,4-dihydroxyphenyl-L-alanine (L-DOPA) contains the catechol moiety which has the peculiar property to form stable complexes with metal cations.[14] This property is responsible of the marine mussel ability to attach to hard surfaces in the sea by means of byssus, that is a mixture of proteins rich in DOPA.[15] The adhesion strength of byssus is also given by the ability to remove interfacial water from the target surfaces.[16]

Although various synthetic DOPA containing hydrogels have been reported, they are constituted by polymeric materials, whose gelation process is activated by high pressure,[17] high temperature,[18] large change in the pH value,[19] and redox reagents.[20]

(4*R*,5*S*)-4-Methyl-5-carboxy-oxazolidin-2-one moiety (D-Oxd) can be successfully utilized in the formation of several supramolecular materials,[21–23] including hydrogels.[24–26] This little molecule, that mimics a proline group, may form oligomers having stable secondary structures in solution, due to its ability to block the peptide bond always in the *trans* conformation.[27–29] Recently, we reported the gelation behavior of Fmoc-protected dipeptides, all containing the D-Oxd moiety and we demonstrated that good results may be obtained with dipeptides containing L-Phe or L-Tyr.[30,31]

In this paper we describe the preparation of physical hydrogels [32–35] using as gelator the L-DOPA containing pseudopeptide **A** (Figure 1). We also compare its ability to form supramolecular hydrogels with L-Phe and L-Tyr containing gelators **B** and **C**.

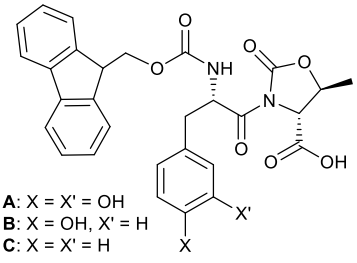

Figure 1. Chemical structure of the three gelators **A**, **B** and **C** described in this work.

Experimental Section

Materials - All chemicals and solvents were purchased by Sigma-Aldrich, VWR or Iris Biotech and used as received. Acetonitrile was distilled under inert atmosphere before use. MilliQ water (Millipore, resistivity = 18.2 mΩ.cm) was used throughout. Solvent were dried by distillation before use. All reaction were carried out in dried glassware. The melting points of the compounds are uncorrected. High quality infrared spectra (64 scans) were obtained with an ATR-FT-IR Bruker Alpha System spectrometer (64 scans). The spectra were obtained in 3 mM solutions in dichloromethane or as solids at 297 K. All compounds were dried *in vacuo* and all the sample preparations were performed in a nitrogen atmosphere. NMR spectra were recorded with a Varian Inova 400 spectrometer at 400 MHz (^{1}H NMR) and 100 MHz (^{13}C NMR). Chemical shifts are reported in δ values relative to the solvent peak.

Boc-L-DOPA-OMe - The molecule was prepared and characterized according to ref. [36]

Boc-L-DOPA(OBn)$_2$-OH - The molecule was prepared and characterized according to ref. [36]

Boc-L-DOPA(OBn)$_2$-D-Oxd-OBn - To a stirred solution of Boc-L-DOPA(OBn)$_2$-OH (466 mg; 0.98 mmol) and HBTU (400 mg, 1.07 mmol) dissolved in dry acetonitrile (10 mL), under inert atmosphere, H-D-Oxd-OBn (229 mg, 0.98 mmol) dissolved in dry acetonitrile (5 mL) was added at room temperature, together with a solution of DIPEA (349 µL, 2.05 mmol). The reaction was monitored by thin layer chromatography; when the reaction was complete, acetonitrile was removed under reduced pressure. Then the crude mixture was dissolved in dichloromethane (30 mL) and washed with water (30 mL), 1 N aqueous HCl (30 mL) and 5% aqueous $NaHCO_3$ (30 mL), dried over anhydrous Na_2SO_4, filtered and evaporated *in vacuo*. The obtained solid was dissolved in methanol (10 mL), ultrasonicated for 15 minutes then filtered over Gooch flask. The solid was washed with methanol (1 x 20 mL), dissolved in dichloromethane to recover it from the filter and evaporated *in vacuo* to afford Boc-L-DOPA(OBn)$_2$-D-Oxd-OBn (576 mg, 0.83 mmol) as a white solid (85 % yield).

M.p. = 171.6-172.0 °C; IR (3 mM in CH_2Cl_2): ν 3439, 1791, 1754, 1711, 1508, 1496 cm^{-1}; ^{1}H NMR (400 MHz, $CDCl_3$): δ 1.36 (d, *J*=6.4 Hz, 3H, CH_3 Oxd), 1.40 (s, 9H, *t*-Bu), 2.81–2.94 (m, 1H, C*H*Hβ-DOPA), 2.96–3.09 (m, 1H, CH*H*β-DOPA), 4.25 (d, *J*=3.9 Hz, 1H, CHN Oxd), 4.43–4.56 (m, 1H, CHO Oxd), 5.11 (s, 2H, CH_2Ph), 5.14 (s, 2H, CH_2Ph), 5.21 (s, 2H, CH_2Ph), 5.78 (s, 1H, CHα-DOPA), 6.69 (d, *J*=8.2 Hz, 1H, CH Ar DOPA), 6.75–6.96 (m, 2H, CH Ar DOPA), 7.14–7.58 (m, 15H, ArH). ^{13}C NMR (100 MHz, $CDCl_3$): δ 21.1, 28.4, 38.8, 53.9, 61.9, 68.1, 71.3, 71.4, 73.6, 79.9, 115.1, 116.4, 122.5, 127.3, 127.6, 127.8, 127.9, 128.4, 128.5, 128.8, 129.1, 134.7, 137.3, 137.4, 148.2, 149.0, 151.2, 154.7,

167.5, 172.7. Anal. Calcd. for $C_{50}H_{44}N_2O_9$: C, 73.52; H, 5.43; N, 3.43. Found: C, 73.48; H, 5.41; N, 3.39.

Fmoc-L-DOPA(OBn)$_2$-D-Oxd-OBn - Trifluoroacetic acid (1.14 mL, 14.40 mmol) was added under nitrogen atmosphere to a solution of Boc-L-DOPA(OBn)$_2$-D-Oxd-OBn (558 mg, 0.80 mmol) in dry dichloromethane (5 mL). After 4 hours the reaction was complete, dichloromethane was removed under reduced pressure and H-L-DOPA(OBn)$_2$-D-Oxd-OBn·CF_3CO_2H was obtained in quantitative yield. The crude was dissolved in dichloromethane (20 mL), then Fmoc *N*-hydroxysuccinimmide ester (270 mg, 0.80 mmol) and DIPEA (516 µL, 3.04 mmol) were added to the mixture, that was stirred at room temperature for 24 hours. Then dichloromethane (30 mL) was added to the mixture, that was washed with water (30 mL), 1 N aqueous HCl (30 mL) and 5% aqueous $NaHCO_3$ (30 mL), dried over anhydrous Na_2SO_4, filtered and evaporated *in vacuo*. The obtained solid was dissolved in methanol (10 mL), ultrasonicated for 15 minutes then filtered over Gooch flask. The solid was washed with methanol (1 x 20 mL), dissolved in dichloromethane to recover it from the filter and evaporated *in vacuo* to afford Fmoc-L-DOPA(OBn)$_2$-D-Oxd-OBn (630 mg, 0.77 mmol) as a white solid (96% yield). M.p. = 160.1-160.3°C; IR (3 mM in CH_2Cl_2): ν 3428, 1792, 1754, 1712, 1511 cm^{-1}; ^{1}H NMR (400 MHz, $CDCl_3$): δ 1.38 (d, *J*=6.4 Hz, 3H, CH_3 Oxd), 2.88–2.98 (m, 1H, C*H*Hβ-DOPA), 3.02–3.13 (m, 1H, CH*H*β-DOPA), 4.14–4.23 (m, 1H, O-C*H*-CH_2-Fmoc), 4.23–4.33 (m, 2H, O-CH-C*H*$_2$-Fmoc), 4.33-4.43(m, 1H, CHN Oxd), 4.48–4.57 (m, 1H, CHO Oxd), 5.08 (s, 2H, CH_2Ph), 5.12 (s, 2H, CH_2Ph), 5.19 (s, 2H, CH_2Ph), 5.41 (d, *J*=8.6 Hz, 1H, NH DOPA), 5.87 (dd, *J*=14.4, 8.6 Hz, 1H, CHα-DOPA), 6.69 (dd, *J*=8.1, 2.0 Hz, 1H, CH Ar DOPA), 6.83 (d, *J*=8.1 Hz, 1H, CH Ar DOPA), 6.87 (d, *J*=2.0 Hz, 1H, CH Ar DOPA), 7.18–7.50 (m, 19H, ArH), 7.55 (d, *J*=6.3 Hz, 2H, ArH Fmoc), 7.75 (d, *J*=6.3 Hz, 2H, ArH Fmoc); ^{13}C NMR (100 MHz, $CDCl_3$): δ 21.2, 38.6, 47.2, 54.3, 61.9, 67.2, 68.2, 71.4, 71.4, 73.8, 115.1, 116.4, 120.0, 122.5, 125.3, 127.2, 127.3, 127.3, 127.5, 127.6, 127.8, 127.8, 127.9, 128.4, 128.5, 128.6, 128.8, 128.8, 134.6, 137.3, 137.4, 141.4, 144.0, 148.4, 149.1, 151.3, 167.4, 172.4. Anal. Calcd. for $C_{40}H_{42}N_2O_9$: C, 69.15; H, 6.09; N, 4.03. Found: C, 69.18; H, 6.08; N, 4.07.

Fmoc-L-DOPA-D-Oxd-OH A - To a stirred solution of Fmoc-L-DOPA(OBn)$_2$-D-Oxd-OBn (100 mg, 0.12 mmol) in a mixture of TFA:methanol 5:95 (100 mL), Pd/C (10% w/w, 10 mg) was added, then vacuum was created inside the flask using the vacuum line. The flask was then filled with hydrogen using a balloon (1 atm). The solution was stirred for 90 minutes under hydrogen atmosphere. The mixture was then filtered and evaporated *in vacuo*, the solid was dissolved in dichloromethane, sonicated and filtrated over Gooch flask. The desired product Fmoc-L-DOPA-D-Oxd-OH was

dissolved in methanol to recover it from the filter and evaporated *in vacuo* and was obtained as a white solid in 85% yield (56 mg, 0.104 mmol).

M.p. = 135.4-136.4°C; IR (ATR-IR): ν 3325, 1783, 1689, 1604, 1517 cm^{-1}; ^{1}H NMR (400 MHz, CD_3OD): δ 1.44 (d, *J*=6.4 Hz, 3H, CH_3 Oxd), 2.75 (dd, *J*=13.5, 5.3 Hz, 1H, CH_2β-DOPA), 3.01 (dd, *J*=13.5, 5.4 Hz, 1H, CH_2β-DOPA), 4.10–4.22 (m, 2H, O-CH-C*H*$_2$-Fmoc), 4.23–4.33 (m, 1H, O-C*H*-CH_2-Fmoc), 4.37 (d, *J*=3.7 Hz, 1H, CHN Oxd), 4.62–4.73 (m, 1H, CHO Oxd), 5.76 (dd, *J*=9.0, 5.3 Hz, 1H, CHα-DOPA), 6.62 (d, *J*=8.3 Hz, 1H, CH-Ar DOPA), 6.67 (d, *J*=8.3 Hz, 1H, CH-Ar DOPA), 6.78 (s, 1H, CH-Ar DOPA), 7.22–7.33 (m, 2H, ArH Fmoc), 7.33–7.41 (m, 2H, Ar-H Fmoc), 7.59 (d, *J*=7.6 Hz, 2H, Ar-H Fmoc), 7.77 (d, *J*=7.7 Hz, 2H, A-rH Fmoc); ^{13}C NMR (100 MHz, CD_3OD): δ 21.2, 30.7, 38.9, 39.2, 56.1, 63.3, 68.1, 75.9, 116.2, 117.5, 120.7, 120.8, 122.1, 125.0, 126.2, 126.3, 127.9, 128.1, 128.6, 129.2, 142.4, 145.1, 145.2, 145.3, 146.1, 153.6, 157.9, 171.5, 174.1. Anal. Calcd. for $C_{19}H_{24}N_2O_9$: C, 53.77; H, 5.70; N, 6.60. Found: C, 53.73; H, 5.75; N, 6.62.

Conditions for the Gel Formation with pH Trigger - 20 mg of compound **A, B** or **C** was placed in a test tube (diameter: 8 mm), then MilliQ water (≈0.95 mL) and aqueous NaOH 1 N (1 equiv.) were added to get a final volume of 1 mL and the mixture was stirred and sonicated in turn for about 30 minutes, until sample dissolution. Then glucono-δ-lactone (GdL: 1.1 equiv.) was added in one portion to the mixture. After a rapid mixing to allow the GdL complete dissolution, the sample was allowed to stand quiescently until gel formation.

Conditions for Gel Formation with Inorganic Triggers - 20 mg of compound **A, B** or **C** was placed in a test tube (diameter: 8 mm), then MilliQ water (0.5 mL) and a 1M aqueous NaOH (1 equiv.) were added to get a final volume of 1 mL. The mixture was stirred until sample dissolution. The cationic trigger (0.3 equiv.) was added to the solution under rapid stirring then the tube was allowed to stand quiescently until gel formation.

Conditions for Gel Formation with Amino Acid Triggers - 20 mg of compound **A, B** or **C** was placed in a test tube (diameter: 8 mm), then the selected amino acid (1 equiv.) was added. 1 mL of MilliQ water was added to the test tube under stirring, then after 1 minute the magnetic stirrer removed and the tube was allowed to stand quiescently until gel formation.

Conditions for T_{gel} Determination - T_{gel} was determined by heating some test tubes (diameter: 8 mm) containing the gel and a glass ball (diameter: 5 mm, weight: 165 mg) on the top of it. When the gel is formed, the ball is suspended atop. The T_{gel} is the temperatures in which the ball start to penetrate inside the gel. Some hydrogel samples melt, producing a clear solution, while in other cases the gelator shrinks and water is ejected, as syneresis occurs.

Aerogels Preparation - The aerogels were prepared with the following procedure: 0.5 mL of the hydrogel was prepared directly into an Eppendorf test tube at room temperature. After the hydrogel is formed (test tube inversion), the sample was deeped in liquid nitrogen for 10 minutes, then it was freeze-dried for 24 hours *in vacuo* (0.02 mBar) at -50 °C using a BENCHTOP Freeze Dry System CHRIST Alpha 1-2 LD Plus.

SEM Analysis - Scanning electron micrographs of the samples were recorded using a Hitachi 6400 field emission gun scanning electron microscope.

Rheology - Rheology experiments were carried out on an Anton Paar Rheometer MCR 102 using a parallel plate configuration (25 mm diameter). Experiments were performed at constant temperature of 25 °C controlled by the integrated Peltier system and a Julabo AWC100 cooling system. To keep the sample hydrated, a solvent trap was used (H-PTD200). Amplitude and Frequency sweep analysis were performed with fixed gap value of 1 mm on gel samples prepared directly on the upper plate of the rheometer. The samples were prepared the day before the analysis and left overnight at controlled temperature of 20 °C to complete the gelation process. Oscillatory amplitude sweep experiments (γ: 0.01−100%) were carried out in order to determine the linear viscoelastic (LVE) range at fixed frequency of 1 rad s^{-1}. Once established the LVE of each hydrogel, frequency sweep tests were performed (ω: 0.1-100 rad·s^{-1}) at constant strain within the LVE region of each sample. To verify the thixotropic properties of the hydrogels strain values within and over the crossover point region where consecutively applied to the hydrogels. The values of the applied strain were selected on the basis of the crossover point value obtained from amplitude sweep experiment for hydrogels **1-9**.

Results and Discussion

Synthesis of Gelator A

The synthesis of gelator **A** started from the unprotected and commercially available L-DOPA that was transformed in five steps into Boc-L-DOPA$(OBn)_2$-OH in multigram scale with excellent yields, following a reported literature.[36,37] Further steps allowed us to introduce the D-Oxd moiety, to replace the Boc moiety with the Fmoc moiety and to remove the three benzyl protecting groups (Scheme 1). The gelator **A** was obtained pure as a white solid in 67% overall yield from L-DOPA. Compounds **B** and **C** have been efficiently prepared in multigram scale, following the reported literatures.[30,31]

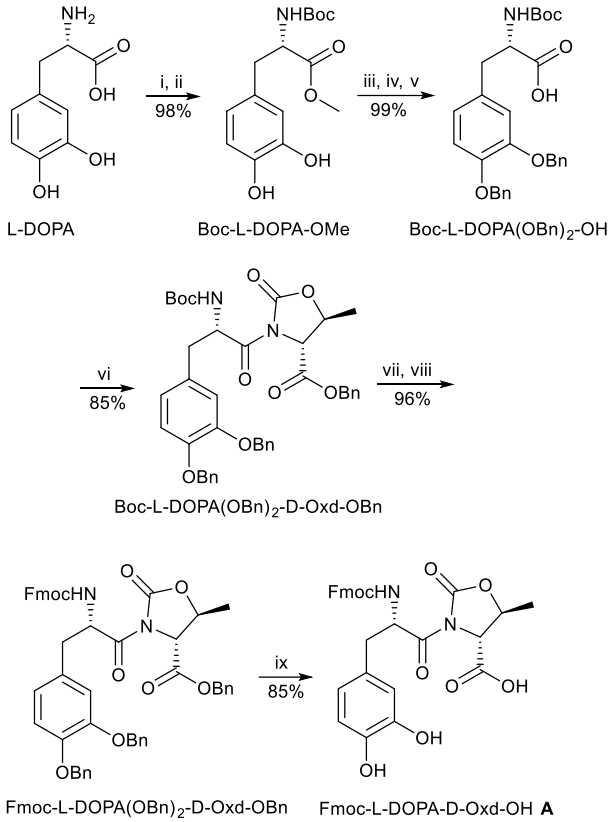

Scheme 1. Reagents and conditions: (i) $SOCl_2$ (excess), MeOH, 0 °C, 24 h; (ii) Boc_2O (2 equiv.), $NaHCO_3$ (2 equiv.), THF/H_2O, r.t., 18 h; (iii) BnBr (2.2 equiv.), K_2CO_3 (2.2 equiv.), TBAB (0.2 equiv.), NaI (0.2 equiv.), acetone, reflux, 4 h; (iv) 1M NaOH, MeOH/THF, r.t., 18 h; (v) 1M HCl; (vi) D-Oxd-OBn (1 equiv.), HBTU (1.1 equiv.), DIEA (2 equiv.), AcCN, r.t., 4 h; (vii) TFA (18 equiv.), CH_2Cl_2, r.t., 4 h; (viii) Fmoc-NHS (1 equiv.), DIEA (3 equiv.), r.t., 24 h; (ix) Pd/C (10% w/w), H_2, MeOH/TFA (95:5), r.t., 90 min.

Hydrogels Formation

A systematic study on the ability of compounds **A**, **B** and **C** to form hydrogels was then undertaken to check the importance of the cresol moiety, as a comparison with a phenol or a phenyl group. The presence of two *ortho*- hydroxyl groups should in principle favour its interaction with metal cations due to their chelation ability. The study of the ability to form metal:peptide complexes with zinc could be of particular interest, as zinc is an essential biological cofactor and plays a critical role in the central nervous system.[38,39] The concentration of intracellular zinc typically ranges between 180 and 250 mM in eukaryotic cells. However, very little zinc exists as 'free' ions within the cell, usually only pico- to low nanomolar concentrations.[40]

We tested the behaviour of zinc cations as triggers to check if they can induce the formation of strong hydrogels with gelators **A**, **B** and **C**. We also compared these results with the behaviour of other triggers: divalent and trivalent metal cations (Ca^{2+}, Ba^{2+}, Mg^{2+}, Cu^{2+}, Al^{3+} and Fe^{3+}) and two

basic amino acids (hystidine and arginine), as we recently demonstrated that they induce the formation of physical hydrogels with selected gelators by coordination with the gelator carboxylate anions.[41,42] We analysed also the hydrogels obtained using the pH variation method as trigger, by addition of a stoichiometric amount of δ-gluconolactone (GdL).[43]

All the hydrogels were prepared with a 2% w/w gelator concentration, that we recognized as the optimal concentration for strong hydrogels formation.[30,41,44] The general method for the hydrogels preparation is to place a portion (20 mg) of gelator **A**, **B** or **C** in a test tube with 1 mL of MilliQ water (for GdL and metal cations triggers a stoichiometric amount of 1M NaOH is also needed). The mixture is stirred until sample dissolution, then the trigger is added to the solution under rapid stirring and the tube is allowed to stand quiescently until gels formation. While a stoichiometric amount of GdL or of a given amino acid is needed for strong gel formation, a stoichiometric trigger/gelator ratio of a metal cation not always provides the best results.[45] We recently demonstrated that a 0.3 trigger/gelator ratio affords strong hydrogels, using calcium chloride as trigger.[42]

We checked if hydrogels are formed under thirty different conditions using **A**, **B** or **C** and ten triggers, but we were able to prepare only eighteen hydrogels. Although we are aware that the modification of the trigger/gelator ratio may afford interesting results, in this preliminary study we chose to screen the triggers only under given conditions to focus the investigation on the gelation efficiency as a function of the hydroxyl groups number. All the trials are summarized in Table 1 and the formed hydrogels have been numbered. All the details are reported in Table S1.

Table 1. Summary of the conditions for hydrogel formation using gelators **A**, **B** and **C**. Only the formed hydrogels have been numbered for clarity.

Gelator → Trigger ↓	Fmoc-L-Dopa-D-Oxd-OH **A**	Fmoc-L-Tyr-D-Oxd-OH **B**	Fmoc-L-Phe-D-Oxd-OH **C**
GdL	**1**	**2**	**3**
$CaCl_2$	**4**	**5**	**6**
$ZnCl_2$	**7**	**8**	**9**
$BaCl_2$	**10**	**11**	-
L-Hys	**13**	**14**	-
$MgCl_2$	-	**17**	**18**
$CuCl_2$	**19**	-	**21**
$Al_2(SO_4)_2$	-	-	-
$Fe(NO_3)_3$	-	-	-
L-Arg	-	-	**30**

GdL, $CaCl_2$ and $ZnCl_2$ allow the formation of hydrogels with any gelator. In contrast $BaCl_2$ and L-Hys result in the formation of hydrogels only with the gelators **A** and **B**, while $MgCl_2$ allow the gelation of only **B** and **C**. Finally, $Al_2(SO_4)_2$, $Fe(NO_3)_3$ and L-Arg furnish unsatisfactory results. Several hydrogels show a thixotropic behaviour at macroscopic scale, as they become liquid if a shear stress is applied then they quickly recover the solid form on resting.[46,47]

Hydrogels Characterization

We have recently demonstrated that good rheological properties are usually associated with higher T_{gel},[30] so a first screening of the optimal conditions for hydrogel formation may be spotted using this method. We measured the T_{gel} for all the eighteen formed hydrogels by the dropping ball method (see Experimental and Table S1 for the details), getting results ranging between 40 °C and 98 °C. Hydrogels **1**-**9**, obtained with GdL, $CaCl_2$ or $ZnCl_2$ have always a T_{gel} higher than 60 °C. Among them, the $ZnCl_2$ containing hydrogels **7**-**9** afford the best results, with T_{gel} always higher than 89 °C. In contrast, no considerable T_{gel} variation may be ascribed to the gelator.

Another interesting parameter that needs to be checked in the hydrogels formation is the final pH, as a neutral pH is very important for the preparation of biocompatible hydrogels. Among the three most interesting triggers, GdL produces the hydrogels **1**-**3** with a pH ranging between 4.0 and 4.5, too low to be biocompatible, although these hydrogels may be very useful for other applications. In contrast, all the other hydrogels have a final pH ranging between 6.5 and 7.5, so they are all good candidates for biological applications.

After this preliminary screening, we focused our attention on hydrogels **1**-**9** that are formed using GdL, $CaCl_2$ or $ZnCl_2$ as gelators. These triggers allow the hydrogels formation with any gelator. The photograph of these hydrogels is shown in Figure 2, while the photographs of all the other hydrogels are reported in Figure S1.

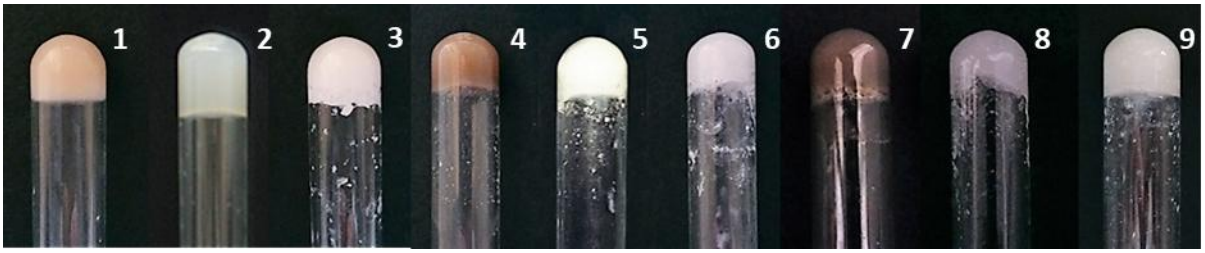

Figure 2. Photographs of hydrogels **1**-**9** (from left to right).

Some more information on the nature of hydrogels **1**-**9** were obtained by SEM analysis of the aerogels prepared by freeze-drying these samples (Figure 3). All the L-DOPA containing aerogels **1**, **4** and **7** are organized in platelets, the L-Tyr containing aerogels **2**, **5** and **8** are organized in dense fibrous networks, finally the L-Phe containing aerogels **3**, **6** and **9** are organized in locally oriented long strips that cross on the large scale. In any case the fast formation of all the hydrogels suggest that the self-assembly occurs under kinetic rather than under thermodynamic conditions.[48,49]

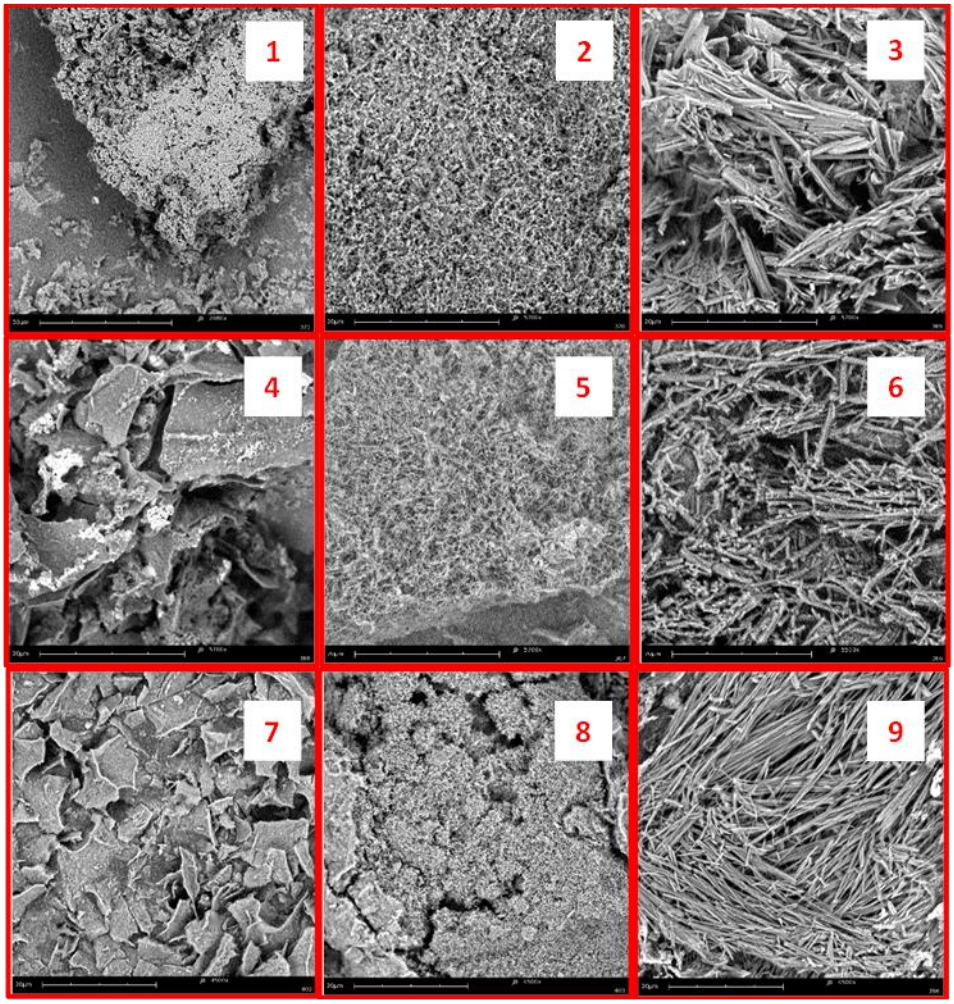

Figure 3. SEM images of samples of xerogel obtained by freeze drying samples of hydrogel **1**-**9**. Bar = 20 µm.

Another piece of information on the supramolecular interactions involved in the formation of hydrogels **1**-**9** may be obtained by the ATR-IR spectra of some aerogels samples. The more ordered fibers obtained with gelator **C** (Figure 4C) produce very reproducible IR spectra, all containing a band at 3330 cm^{-1} typical of hydrogen bonded NH bonds, another strong stretching band at 1687 cm^{-1}, typical of hydrogen bonded CO bonds, together with a weaker band around 1067 cm^{-1} that

may be attributed to the amide band II. The dense fibrous networks, typical of aerogels **2**, **5** and **8** show a more complex pattern (Figure 4B), where prevails either band I at about 1690 cm^{-1} or band II at about 1600 cm^{-1}. Finally the L-DOPA containing aerogels **1**, **4** and **7** (Figure 4A) have IR spectra where both amide band I and amide band II are present, together with the NH stretching band at 3325 cm^{-1}.

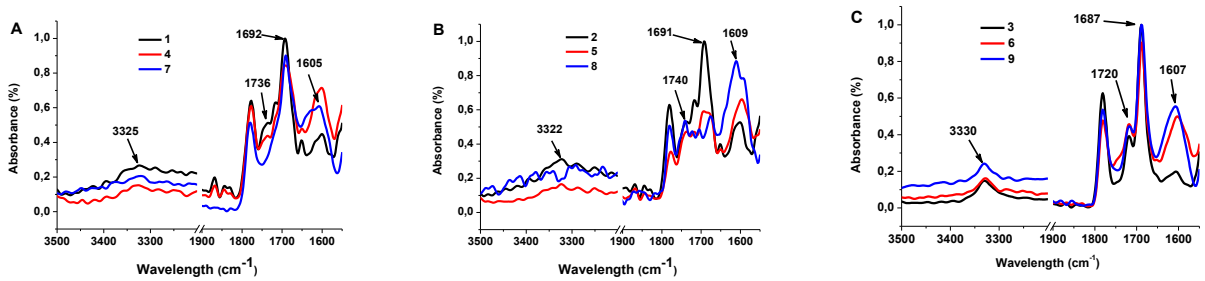

Figure 4. Selected regions of ATR-IR spectra of aerogels **1**-**9**: (A) L-DOPA containing aerogels **1**, **4** and **7**; (B) L-Tyr containing aerogels **2**, **5** and **8**; (C) L-Phe containing aerogels **3**, **6** and **9**.

Rheological analyses have been carried out to evaluate the viscoelastic properties of hydrogels **1**-**9** in terms of storage and loss moduli (G' and G" respectively) (Table 2, Figures S3-S5). All the obtained hydrogels are characterized by a storage modulus approximately an order of magnitude higher than the loss component, indicating their "solid-like" attitude. Frequency sweep analysis pointed out that for all the obtained hydrogels both G' and G" were almost independent from the frequency in the range from 0.1 to 100 $rad \cdot s^{-1}$ (with G' always greater than G") confirming the "solid-like" rheological behaviour.

Table 2. Rheological properties of hydrogels **1**-**9**.

Hydrogel	Gelator	Trigger (equiv.)	G'(Pa)	G''(Pa)	γ (%)
1	**A**	GdL (1.1)	3400	430	9.64
2	**B**	GdL (1.1)	52600	5000	11.55
3	**C**	GdL (1.1)	48800	3440	3.22
4	**A**	$CaCl_2$ (0.3)	8500	1050	6.65
5	**B**	$CaCl_2$ (0.3)	17000	2500	5.42
6	**C**	$CaCl_2$ (0.3)	6400	430	12.76
7	**A**	$ZnCl_2$ (0.3)	2144	366	3.88
8	**B**	$ZnCl_2$ (0.3)	74271	7280	4.69
9	**C**	$ZnCl_2$ (0.3)	700	61	6.00

Rheological studies indicate that the strength of the hydrogels is strongly affected both by the aromatic amino acid and by the trigger. The general trends demonstrate that, maintaining a 0.3 trigger/gelator ratio, the strongest gels are obtained with the L-Tyr containing gelator **B**, as hydrogels **2**, **5** and **8** are characterized by storage modulus G' values ranging between 10^4 and 10^5 Pascal, with the hydrogels strength following the trend $ZnCl_2$ > GdL > $CaCl_2$. The L-DOPA containing hydrogels **1**, **4** and **7** are characterized by storage modulus approximately an order of magnitude lower, always ranging between 10^3 and 10^4 Pascal, with the hydrogels strength following the trend $CaCl_2$ > GdL > $ZnCl_2$. This unexpected result may be ascribed to the trigger/gelator ratio that could be more suitable for gelator **B** rather than for the cresol containing gelator **A**. We are planning to study the effect of the variation of the trigger/gelator ratio on the hydrogel properties when gelator **A** is used.

Finally, the L-Phe containing gelator **C**, that does not possess hydroxyl groups, is very sensitive towards the trigger, as the hydrogels strength follow the trend GdL > $CaCl_2$ > $ZnCl_2$. These results indicate that there is not a universal trigger able to induce the formation of a hydrogel endowed with the best mechanical properties.

Step strain experiments were performed to check the thixotropic behaviour of hydrogels **1**-**9** at the molecular level. Strain values within and over the crossover point region where consecutively applied to the hydrogels, that lose their "solid-like" behavior (G'<G") when the strain applied is over their crossover point region and quickly go back to a "solid-like" state (G'>G") if the strain is in the LVE region the hydrogels (Figure 5).

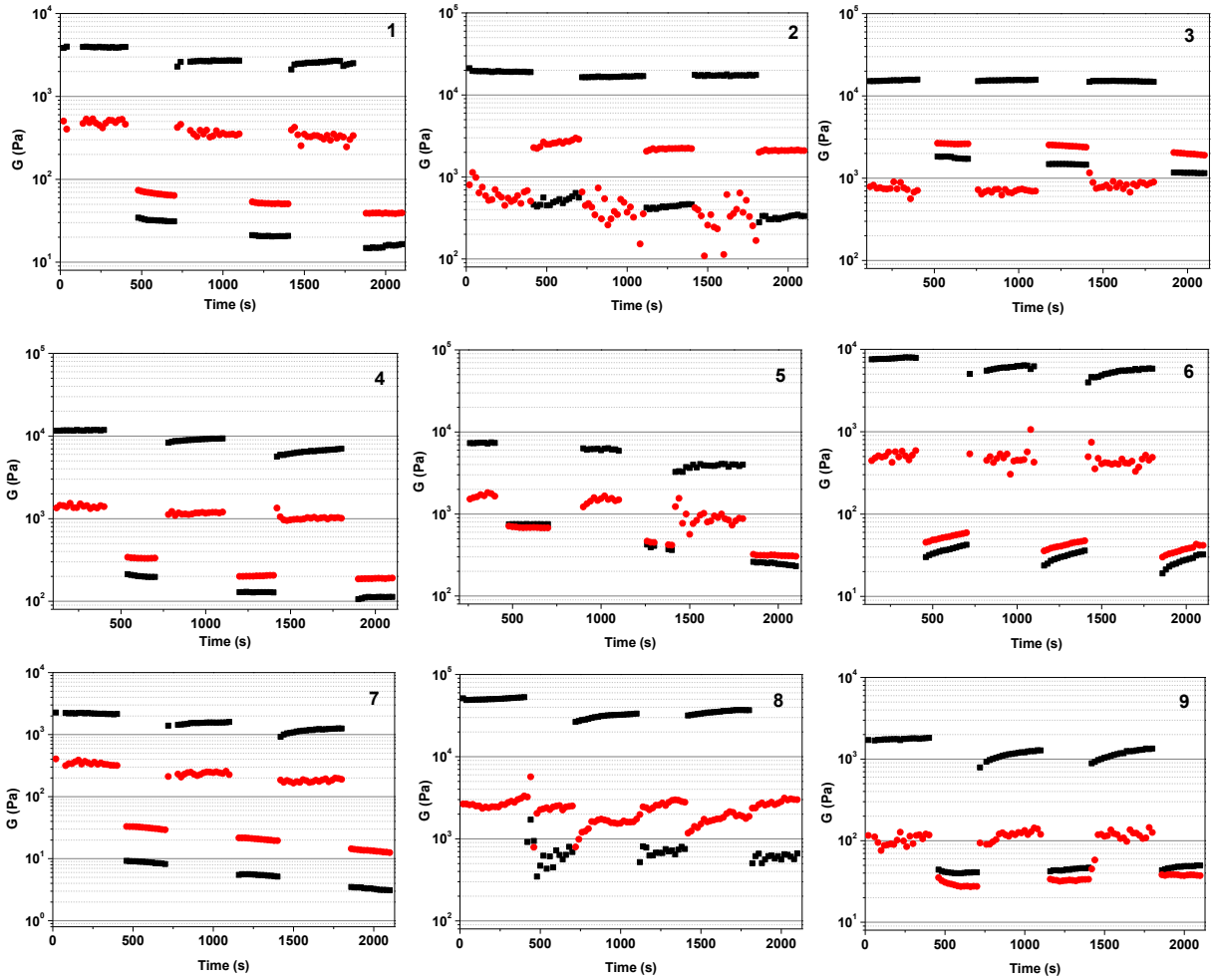

Figure 5. Values of storage moduli G' (black) and loss moduli G" (red) recorded during a step strain experiment performed on hydrogels **1**-**9**.

Although only hydrogels **3**, **6**, **7**, **8** and **9** show a thixotropic behaviour at macroscopic scale (Table S1), the results observed for hydrogels **1**-**9** show that they are all characterized by a great capability to recover the gel-like behaviour, thus showing their thixotropic properties at the molecular level.

Conclusions

We prepared the new gelator Fmoc-L-DOPA-D-Oxd-OH **A** and we tested its gelation ability as a comparison with the already reported gelators Fmoc-L-Tyr-D-Oxd-OH **B** and Fmoc-L-Phe-D-Oxd-OH **C** under several gelation conditions, to check the effect of the cresol moiety.

As an overall observation, the different gelators behaviour may be attributed to the increased water solubility of the L-DOPA and L-Tyr derivatives compared with the L-Phe containing gelator. The results obtained with the ten different triggers indicate that the hydrogel formation is very sensitive both to the number of the hydroxyl moieties linked to the aromatic rings and to the trigger nature, so there is not a universal trigger able to produce the hydrogel with the best mechanical properties in any case.

GdL, $CaCl_2$ and $ZnCl_2$ form strong hydrogels endowed with thixotropic behaviour at the molecular level with all the three gelators. The analysis of the aerogels obtained by freeze drying the hydrogels show that the three gelators induce the formation of dense networks, as the **A** aerogels show a platelet pattern, the **B** aerogels display an unordered dense fibrous network and the **C** aerogels are organized in locally oriented long strips. The rheological analysis of these samples demonstrate that the strongest hydrogels are obtained with the L-Tyr containing gelator **B**, while the L-DOPA containing hydrogels **1**, **4** and **7** are characterized by a storage modulus approximately an order of magnitude lower. Finally, the strength of L-Phe containing hydrogels show a different trigger dependency respect to the other ones.

Although the fast formation of all the hydrogels suggest that the self-assembly occurs under kinetic rather than under thermodynamic conditions, more studies are planned to have a deeper understanding in the hydrogelation process that could be responsible for the formation of stronger hydrogels with the L-Tyr gelator **B** compared to the gels formed by the L-DOPA gelators **A**. Moreover, the variation of the trigger/gelator ratio may modify these results, as a different amount of Ca^{2+} or Zn^{2+} could be more suitable for hydrogels formation in the presence of the cresol moiety.

Finally, the strong $ZnCl_2$ containing hydrogels **7**-**9**, suggest that the three gelators have a good propensity to form complexes with this metal. Further studies are currently ongoing to find the optimal gelator/$ZnCl_2$ ratio for the formation of strong and thixotropic hydrogels for biological and cell growth applications.

Acknowledgements

We gratefully acknowledge Ministero dell'Università e della Ricerca (PRIN 2015 project 20157WW5EH) and Alma Mater Studiorum Università di Bologna for financial support.

References

1 S. Guha, M. G. B. Drew and A. Banerjee, *Chem. Mater.*, 2008, **20**, 2282–2290.

2 S. K. Maji, D. Haldar, A. Banerjee and A. Banerjee, *Tetrahedron*, 2002, **58**, 8695–8702.

3 S. K. Maji, M. G. Drew and A. Banerjee, *Chem. Commun.*, 2001, 1946–1947.

4 R. V Ulijn and A. M. Smith, *Chem. Soc. Rev.*, 2008, **37**, 664–675.

5 F. Rúa, S. Boussert, T. Parella, I. Díez-Pérez, V. Branchadell, E. Giralt and R. M. Ortuño, *Org. Lett.*, 2007, **9**, 3643–3645.

6 T. A. Martinek, A. Hetényi, L. Fulop, I. M. Mándity, G. K. Tóth, I. Dékány and F. Fülöp, *Angew. Chemie - Int. Ed.*, 2006, **45**, 2396–2400.

7 Q. Zou, M. Abbas, L. Zhao, S. Li, G. Shen and X. Yan, *J. Am. Chem. Soc.*, 2017, **139**, 1921–1927.

8 M. Abbas, Q. Zou, S. Li and X. Yan, *Adv. Mater.*, 2017, **29**.

9 K. Liu, R. Xing, Q. Zou, G. Ma, H. Mohwald and X. Yan, *Angew. Chemie - Int. Ed.*, 2016, **55**, 3036–3039.

10 X. Liu, J. Fei, A. Wang, W. Cui, P. Zhu and J. Li, *Angew. Chemie Int. Ed.*, 2017, **56**, 2660–2663.

11 F. E. Cohen and J. W. Kelly, *Nature*, 2003, **426**, 905–909.

12 J. Sato, T. Takahashi, H. Oshima, S. Matsumura and H. Mihara, *Chem. - A Eur. J.*, 2007, **13**, 7745–7752.

13 R. Mishra, B. Bulic, D. Sellin, S. Jha, H. Waldmann and R. Winter, *Angew. Chemie - Int. Ed.*, 2008, **47**, 4679–4682.

14 A. Fernandez-Barbero, I. J. Suarez, B. Sierra-Martin, A. Fernandez-Nieves, F. J. de las Nieves, M. Marquez, J. Rubio-Retama and E. Lopez-Cabarcos, *Adv. Colloid Interface Sci.*, 2009, **147–148**, 88–108.

15 Y. Liu, H. Meng, Z. Qian, N. Fan, W. Choi, F. Zhao and B. P. Lee, *Angew. Chemie Int. Ed.*, 2017, **56**, 4224–4228.

16 P. Kord Forooshani and B. P. Lee, *J. Polym. Sci. Part A Polym. Chem.*, 2017, **55**, 9–33.

17 Z. Q. Lei, H. P. Xiang, Y. J. Yuan, M. Z. Rong and M. Q. Zhang, *Chem. Mater.*, 2014, **26**, 2038–2046.

18 X. Dai, Y. Zhang, L. Gao, T. Bai, W. Wang, Y. Cui and W. Liu, *Adv. Mater.*, 2015, **27**, 3566–3571.

19 Y. Hu, W. Guo, J. S. Kahn, M. A. Aleman-Garcia and I. Willner, *Angew. Chemie - Int. Ed.*, 2016, **55**, 4210–4214.

20 M. Nakahata, Y. Takashima, H. Yamaguchi and A. Harada, *Nat. Commun.*, 2011, **2**, 1–6.

21 G. Angelici, N. Castellucci, G. Falini, D. Huster, M. Monari and C. Tomasini, *Cryst. Growth Des.*, 2010, **10**, 923–929.

22 G. Angelici, G. Falini, H. J. Hofmann, D. Huster, M. Monari and C. Tomasini, *Chem. - A Eur. J.*, 2009, **15**, 8037–8048.

23 G. Angelici, N. Castellucci, S. Contaldi, G. Falini, H. J. Hofmann, M. Monari and C. Tomasini, *Cryst. Growth Des.*, 2010, **10**, 244–251.

24 N. Castellucci, G. Sartor, N. Calonghi, C. Parolin, G. Falini and C. Tomasini, *Beilstein J. Org. Chem.*, 2013, **9**, 417–424.

25 N. Castellucci, G. Angelici, G. Falini, M. Monari and C. Tomasini, *European J. Org. Chem.*, 2011, 3082–3088.

26 N. Castellucci, G. Falini, G. Angelici and C. Tomasini, *Amino Acids*, 2011, **41**, 609–620.

27 S. Lucarini and C. Tomasini, *J. Org. Chem.*, 2001, **66**, 727–732.

28 C. Tomasini, V. Trigari, S. Lucarini, F. Bernardi, M. Garavelli, C. Peggion, F. Formaggio and C. Toniolo, *European J. Org. Chem.*, 2003, **4**, 259–267.

29 G. Angelici, G. Luppi, B. Kaptein, Q. B. Broxterman, H. J. Hofmann and C. Tomasini, *European J. Org. Chem.*, 2007, 2713–2721.

30 N. Zanna, A. Merlettini, G. Tatulli, L. Milli, M. L. Focarete and C. Tomasini, *Langmuir*, 2015, **31**, 12240–12250.

31 L. Milli, N. Castellucci and C. Tomasini, *European J. Org. Chem.*, 2014, 5954–5961.

32 K. L. Morris, L. Chen, A. Rodger, D. J. Adams and L. C. Serpell, *Soft Matter*, 2015, **11**, 1174–1181.

33 G. Fichman and E. Gazit, *Acta Biomater.*, 2014, **10**, 1671–1682.

34 B. Adhikari, J. Nanda and A. Banerjee, *Chem. - A Eur. J.*, 2011, **17**, 11488–11496.

35 L. Chen, K. Morris, A. Laybourn, D. Elias, M. R. Hicks, A. Rodger, L. Serpell and D. J. Adams, *Langmuir*, 2010, **26**, 5232–5242.

36 A. Gaucher, L. Dutot, O. Barbeau, W. Hamchaoui, M. Wakselman and J. P. Mazaleyrat, *Tetrahedron Asymmetry*, 2005, **16**, 857–864.

37 G. E. Magoulas, A. Rigopoulos, Z. Piperigkou, C. Gialeli, N. K. Karamanos, P. G. Takis, A. N. Troganis, A. Chrissanthopoulos, G. Maroulis and D. Papaioannou, *Bioorg. Chem.*, 2016, **66**, 132–144.

38 K. L. Veldkamp, P. J. Tubergen, M. A. Swartz, J. T. DeVries and C. D. Tatko, *Inorganica Chim. Acta*, 2017, **461**, 120–126.

39 F. Burnett, *Lancet*, 1981, **317**, 186–188.

40 R. D. Palmiter and S. D. Findley, *EMBO J.*, 1995, **14**, 639–649.

41 N. Zanna, A. Merlettini and C. Tomasini, *Org. Chem. Front.*, 2016, **3**, 1699–1704.

42 N. Zanna, S. Focaroli, A. Merlettini, L. Gentilucci, G. Teti, M. Falconi and C. Tomasini, *ACS Omega*, 2017, **2**, 2374−2381.

43 D. J. Adams, M. F. Butler, W. J. Frith, M. Kirkland, L. Mullen and P. Sanderson, *Soft Matter*, 2009, **5**, 1856–1862.

44 L. Milli, N. Zanna, A. Merlettini, M. Di Giosia, M. Calvaresi, M. L. Focarete and C. Tomasini, *Chem. - A Eur. J.*, 2016, 12106–12112.

45 L. Chen, G. Pont, K. Morris, G. Lotze, A. Squires, L. C. Serpell and D. J. Adams, *Chem. Commun.*, 2011, **47**, 12071–3.

46 Y. Li, F. Zhou, Y. Wen, K. Liu, L. Chen, Y. Mao, S. Yang and T. Yi, *Soft Matter*, 2014, **10**, 3077–85.

47 J. Mewis and N. J. Wagner, *Adv. Colloid Interface Sci.*, 2009, **147**–**148**, 214–227.

48 J. Wang, K. Liu, L. Yan, A. Wang, S. Bai and X. Yan, *ACS Nano*, 2016, **10**, 2138–2143.

49 J. Wang, K. Liu, R. Xing and X. Yan, *Chem. Soc. Rev.*, 2016, **45**, 5589–5604.